A Time-Dependent Model of the Upper Ocean[1]

K. L. DENMAN[2]

Institute of Oceanography, University of British Columbia, Vancouver 8, Canada

(Manuscript received 28 August 1972, in revised form 15 December 1972)

ABSTRACT

A model describing the time-dependent modification of the upper mixed layer of the ocean by meteorological influences is developed. The turbulent mixing and the radiative heating within the mixed layer are expressed so that only simple parameters available from routine meteorological measurements are required as input. The model is sensitive to the rate of production by the wind stress of energy available for mixing, and to the rate of absorption with depth of the solar radiation. Analytic and numerical results of the model for conditions of large constant winds and typical summer heating are consistent with laboratory results. The mixing response to a wind normally distributed in time is also presented. Finally, the model simulates the physical behavior of the upper mixed layer in response to diurnally varying heating: results for several different values of wind speed indicate that, even in low winds and typical summer heating, the daily fluctuations in sea surface temperature in the open ocean should seldom exceed 0.2C.

1. Introduction

Recent works concerned with long-range atmospheric prediction, such as those of Namias (1969, 1970), Manabe (1969) and Bryan (1969), indicate that the climate and its fluctuations are profoundly influenced by the interaction of the ocean with the atmosphere. Since many atmospheric processes occur over periods of 1–5 days, an understanding of the behavior of the upper ocean on these time scales is basic to the complete understanding of the ocean-atmosphere system.

Although the study of the upper layer of the ocean was pioneered by Ekman (1905), the first realistic model including stratification was that of Munk and Anderson (1948). Using eddy coefficients of viscosity and conductivity which varied with depth according to the vertical gradients of current and temperature (or density), they obtained steady-state solutions for the depth and shape of the thermocline. The eddy coefficient approach has the disadvantage of requiring knowledge of the current shear which, even today, is difficult to measure within the Ekman layer.

Kitaygorodskiy (1961) also formulated a one-dimensional model of the upper layer. By assuming that the current shear was just that of the orbital wave velocities, he was able to calculate the current shear from the measured wave field rather than from actual current measurements. Although he too obtained a (steady-state) solution, he did recognize the necessity of including turbulence in his formulation.

Kraus and Turner (1967) developed a mixed layer model which eliminated the need to use eddy coefficients by considering the layer to be homogeneous: heat inputs to the layer and mass entrained at the bottom of the layer were instantaneously mixed uniformly through the layer. For a sawtooth solar heating function, they were able to obtain a time-dependent solution which explains qualitatively the annual cycle of the buildup and destruction of the seasonal thermocline. In a companion paper (Turner and Kraus, 1967), they obtained similar results with a laboratory model. In both papers, the wind mixing (stirring) was constant; in the theoretical model it was equivalent to the mixing of light winds ($\sim$5 m sec^{-1}).

Kato and Phillips (1969) examined the formation of a homogeneous layer, and the downward mixing of its bottom interface in an annular tank with a rotating stirrer. They found that the rate of increase of potential energy of the stratified fluid was proportional to the rate of dissipation of kinetic energy per unit area in the turbulent layer. Further, for constant stirring and for an initial linear density profile, the thickness of the mixed layer increased as the elapsed time to the one-third power. The findings of Kato and Phillips should be applicable to the open ocean, provided that the rate of work being done against the buoyancy forces by mixing within the homogeneous layer can be accurately estimated.

In this paper, a generalization of the Kraus-Turner model is employed to investigate the time-dependent behavior of the upper mixed layer of the ocean in response to varying meteorological inputs of time scales from one to several days. The characteristic responses

[1] A Bedford Institute of Oceanography contribution.

[2] Present affiliation: Fisheries Research Board of Canada, Marine Ecology Laboratory, Bedford Institute of Oceanography, Dartmouth, Nova Scotia, Canada.

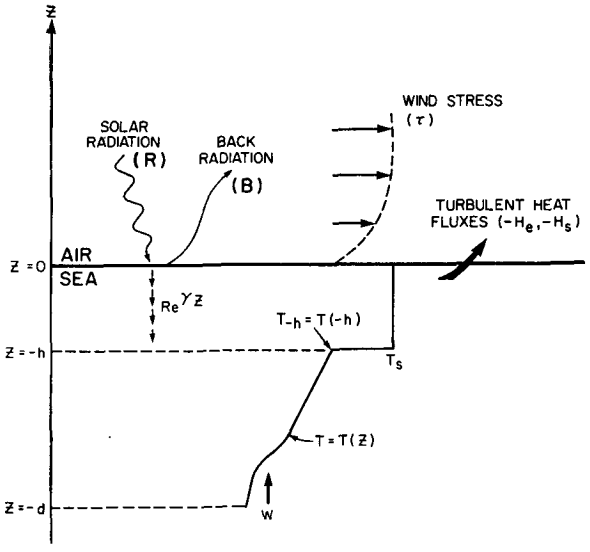

FIG. 1. Schematic of the thermocline and the boundary inputs assumed in the model. The mixed layer parameters are: the thickness h; the temperature T_s; and the extinction coefficient γ, for the incident solar radiation R. Other boundary conditions are the wind stress τ; the back radiation $-B$; the latent and sensible fluxes of heat $-(H_e+H_s)$ at the upper surface; the temperature $T(-h)$, immediately below the layer; and the vertical velocity w below the layer.

of the model to strong winds are examined both analytically and numerically for a constant wind stress with small heat exchanges and for a varying wind normally distributed in time. The case of constant heating with light winds is solved for various rates of absorption of solar radiation. Finally, the response of the upper layer to diurnally varying heating is investigated for several different wind speeds.

In a companion paper (Denman and Miyake, 1973) the model is run with observed values of wind speed, solar radiation, and back radiation obtained for a 2-week period from Ocean Station *Papa* in the northeast Pacific Ocean (50N, 145W). The simulated upper layer structure is compared with frequent observations of salinity, temperature and depth, also obtained at Station *Papa* during the same period.

2. Derivation of the integrated equations

The time-dependent behavior of the upper mixed layer at a single point is formulated in this section. A set of coupled ordinary differential equations are derived from the conservation equations of heat and mechanical energy, and from the appropriate boundary conditions. In the final equations, time derivatives of h (the mixed layer thickness), T_s (the mixed layer temtemperature), and T_{-h} (the temperature immediately below the mixed layer) are expressed in terms of the time-dependent boundary inputs. These inputs include wind stress, solar and back radiation, latent and sensible heat fluxes across the upper boundary, and the temperature gradient below the layer.

a. Assumptions

The ocean is assumed to be an incompressible, stably stratified fluid obeying the Boussinesq approximation. Wave-like dynamical effects such as gravitational, inertial and Rossby waves are ignored. Further, the ocean is assumed to be horizontally homogeneous. Horizontal inhomogeneity can enter only indirectly through divergence (or convergence) within the upper layer resulting from non-zero curl in the large-scale wind stress field.

The upper mixed layer is an idealized, vertically homogeneous layer bounded at the bottom by a density (temperature) discontinuity as shown in Fig. 1. The heat and mechanical energy inputs at the upper and lower boundaries, or at any point within the mixed layer, are assumed to be redistributed uniformly throughout the layer by turbulent diffusion. The times required for this redistribution are small compared to the times over which the processes of interest in this model are assumed to occur.

Below the lower interface, a stable density profile is specified. Also below the mixed layer, an advective vertical velocity w, resulting from the above-mentioned convergence (or divergence) within the upper layer, may be specified at some arbitrary depth, $z=-d(<-h)$.

b. Conservation of thermal energy

If one neglects molecular heat fluxes and viscous generation of heat, then the first law of thermodynamics for an incompressible fluid leads to the following relation for the material rate of change of temperature:

$$\frac{dT}{dt}=Q_T/(\rho c_p) \tag{1}$$

at any level z, where Q_T is a heat source term (due to absorption of radiation), ρ is density, and c_p is the specific heat at constant pressure [taken to be 0.96 cal gm^{-1} (°K)$^{-1}$ for normal sea water].

Since the absorption of solar radiation can be characterized approximately by an average extinction coefficient γ (see Fig. 49 in Jerlov, 1968), the heat source term is just $Q_T=\gamma R_* e^{\gamma z}$ (in units of cal cm^{-3} sec^{-1}), where R_* is the solar radiation incident on the sea surface (cal cm^{-2} sec^{-1}). Substituting the expression for Q_T into the time-averaged turbulent form of (1) gives the heat conservation equation

$$\frac{\partial T}{\partial t}+w\frac{\partial T}{\partial z}+\frac{\partial}{\partial z}\overline{(w'T')}=\frac{\gamma R_* e^{\gamma z}}{\rho_0 c_p}, \tag{2}$$

where $T(z)$ and $T'(z)$ are the mean and fluctuating components of temperature, w is the mean vertical velocity, and ρ_0 the mean density.

The term $\partial(\overline{w'T'})/\partial z$ represents the local divergence of the turbulent flux of heat. It is this term that redistributes the heat exchanged at the boundaries

uniformly throughout the homogeneous layer in a time that is short compared to the time scales of interest in the model (as stated in the assumptions). Within the completely mixed layer the advective term, $w\partial T/\partial z$, of course vanishes.

c. Conservation of mechanical energy

For the case of horizontal homogeneity in the presence of a mean horizontal current u, the equation governing the turbulent kinetic energy of the fluid is (cf. Phillips, 1966)

$$\frac{\partial}{\partial t}\left(\frac{\overline{c^2}}{2}\right)=-\overline{u'w'}\frac{\partial u}{\partial z}-\frac{\partial}{\partial z}\overline{\left[w'\left(\frac{p'}{\rho_0}+\frac{c^2}{2}\right)\right]}-\frac{\overline{w'\rho'}}{\rho_0}g-\epsilon, \quad (3)$$

where $c^2=u'^2+v'^2+w'^2$, ϵ is the rate of dissipation of turbulent energy, g the acceleration due to gravity, p' the pressure fluctuation, and ρ' the density fluctuation, which according to the Boussinesq assumption enters only through buoyancy effects.

The mean kinetic energy of the turbulent motion, $\overline{c^2}/2$, is of order $\frac{3}{2}w_*^2$, where w_* is the friction velocity $(\tau/\rho)^{\frac{1}{2}}$, corresponding to the applied wind stress τ. For winds near 10 m sec^{-1}, $w_*\approx 1$ cm sec^{-1}. For time scales of the order of 1 day, the term $\frac{1}{2}\partial\overline{c^2}/\partial t$ is thus of the order 10^{-5} cm^2 sec^{-3}. On the other hand, a typical value of ϵ within the mixed layer but below the wave breaking zone is of the order 10^{-2} cm^2 sec^{-3} (Grant *et al.*, 1968). Thus, the term $\frac{1}{2}\partial\overline{c^2}/\partial t$ is clearly negligible in (3).

The term $-\overline{u'w'}\partial u/\partial z$ represents the rate of production of turbulent energy by the turbulent Reynolds stresses acting on the mean current shear. The rate of energy loss (in the case of a stably stratified fluid) from the turbulence by work done against the density gradient to increase the potential energy of the mean density field is given by $-\overline{w'\rho'}g/\rho_0$. Finally,

$$-\frac{\partial}{\partial z}\overline{\left[w'\left(\frac{p'}{\rho_0}+\frac{c^2}{2}\right)\right]}$$

represents the local divergence of the vertical transports of the turbulent mechanical energy produced mainly by breaking waves at the upper surface and by the Reynolds stresses acting on the mean flow. As in the case of the divergence term for the turbulent heat flux in (2), the divergence term for mechanical energy is assumed to redistribute the turbulent energy uniformly throughout the layer within a time which is short compared to the times of interest in the model.

The resulting steady-state equation for turbulent mechanical energy is

$$-\overline{u'w'}\frac{\partial u}{\partial z}-\frac{\partial}{\partial z}\overline{\left[w'\left(\frac{p'}{\rho_0}+\frac{c^2}{2}\right)\right]}=\alpha g\overline{w'T'}+\epsilon, \quad (4)$$

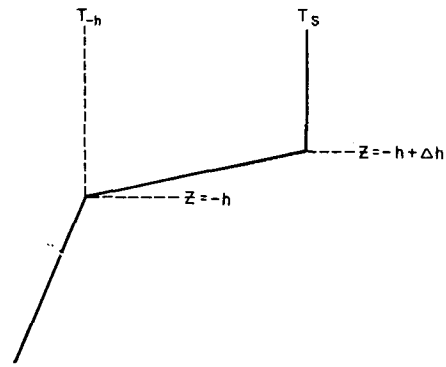

FIG. 2. Enlargement of the interface at the bottom of the mixed layer.

where ρ' has been replaced with T' by use of $d\rho\approx\alpha\rho_0 dT$ (salinity changes are assumed to be small) with $\alpha=\rho_0^{-1}\partial\rho/\partial T$. The terms on the left are the source terms for turbulent mechanical energy; those on the right are the sink terms.

d. The mixing entrainment

To determine the turbulent mixing that occurs in the upper layer as colder, heavier water from below is entrained upward, one must look in detail at the interface between the layers. Consider the interface to have a thickness Δh, as shown in Fig. 2. The average vertical advection velocity of the layer below is w. If the turbulent mixing $\overline{w'T'(z)}$ is assumed to be zero at $z=-h$ immediately below the interface, then (2) can be integrated between $z=-h$ and $z=-h+\Delta h$ to yield the following equation (to first order in Δh):

$$\frac{\partial T}{\partial t}\Delta h+(T_s-T_{-h})\left(w+\frac{\partial h}{\partial t}\right)+\overline{w'T'}\Big|_{-h+\Delta h}=\frac{\gamma R_* e^{-\gamma h}\Delta h}{\rho_0 c_p}. \quad (5)$$

In the limit as $\Delta h\to 0$, Eq. (7) reduces to the following expression for the mixing entrainment at the bottom of the mixed layer:

$$\overline{w'T'}_{-h}=-H\left(w+\frac{dh}{dt}\right)(T_s-T_h), \quad (6)$$

where $\partial h/\partial t$ has been replaced by dh/dt under the assumption of horizontal homogeneity, and H is the Heaviside step function having the properties

$$H=\begin{cases}0, \text{ if } w+\dfrac{dh}{dt}\leqslant 0\text{; no entrainment mixing}\\ \\ 1, \text{ if } w+\dfrac{dh}{dt}>0\text{; entrainment mixing at } z=-h.\end{cases} \quad (7)$$

The Heaviside function H has been introduced so that when the production of turbulent energy within the upper layer is insufficient to maintain entrainment at the bottom interface (say, for low winds and large solar heating), the physically unrealistic situation of "unmixing" does not occur. Eq. (6) was used as the upper boundary condition for a model of the well-mixed atmospheric boundary layer by Geisler and Kraus (1969).

e. The upper boundary

At the top of the mixed layer, the turbulent heat flux must equal the net heat transfer through the ocean surface, i.e.,

$$\overline{w'T'(0)}=-F_*/(\rho_0 c_p), \tag{8}$$

where F_* is the downward flux of heat across the air-sea interface (in units of cal cm^{-2} sec^{-1}). If H_s* and H_e* are the downward fluxes of sensible and latent heat at the sea surface, and $-B_*$ the net heat loss by longwave radiation from the sea surface, then

$$F=H_e+H_s+B, \tag{9}$$

where the transformation

$$(F,R,B,H_e,H_s)=(F_*,R_*,B_*,H_e*,H_s*)/(\rho_0 c_p)$$

has been used.

f. The lower layer

In order to specify the system completely, one must know the temperature gradient $\partial T/\partial z$ below the mixed layer. If the assumption is made that no turbulent energy penetrates below $z=-h$, then the time rate of change of temperature at some depth z (where $-d<z<-h$) is given by the heat conservation equation (2):

$$\frac{\partial T(z)}{\partial t}=\gamma \mathrm{Re}^{\gamma z}-w\frac{\partial T(z)}{\partial z}. \tag{10}$$

At the interface, $z=-h$, the total derivative must be used, i.e.,

$$\frac{d}{dt}T(-h)=\frac{\partial}{\partial t}T(-h)-\frac{dh}{\partial t}\frac{\partial T}{\partial z}\bigg|_{-h}$$
$$=\gamma\,\mathrm{Re}^{-\gamma h}-\left(w+\frac{dh}{dt}\right)\frac{\partial T}{\partial z}\bigg|_{-h}, \tag{11}$$

where use has been made of (10). Here, one assumes that the only local surface influence acting on the ocean at depth $z<-h$ is the small fraction of solar radiation which penetrates to that depth.

g. The mixed layer

Integration of the thermal energy equation (2) over the mixed layer (of uniform temperature T_s) with use of (6) and (8), leads to

$$h\frac{dT_s}{dt}+H\left(w+\frac{dh}{dt}\right)(T_s-T_{-h})=F+R(1-e^{-\gamma h}). \tag{12}$$

Integration of the mechanical energy equation (4) yields

$$-\int_{-h}^{0}\overline{u'w'}\frac{\partial u}{\partial z}dz-\overline{w'\left(\frac{p'}{\rho_0}+\frac{c^2}{2}\right)}\bigg|_{z=0}$$
$$=\alpha g\int_{-h}^{0}\overline{w'T'}dz+\int_{-h}^{0}\epsilon dz, \tag{13}$$

where the mean of $w'[(p'/\rho_0)+(c^2/2)]$ evaluated at $z=-h$ is assumed to be zero. The term $\alpha g\int_{-h}^{0}\overline{w'T'}dz$ can be eliminated by the use of Eq. (2) integrated twice over z (with $w\partial T/\partial z$ once more neglected):

$$\int_{-h}^{0}\overline{w'T'}(z)dz$$
$$=\frac{h^2}{2}\frac{dT_s}{dt}-Fh-R(h-\gamma^{-1})-\gamma^{-1}\mathrm{Re}^{-\gamma h}. \tag{14}$$

If $(G,D)=-(\rho_0\alpha g)^{-1}(G_*,D_*)$ in units of [cm^2 (°K) sec^{-1}], where

$$\left.\begin{aligned}G_*&=-\rho_0\int_{-h}^{0}\overline{u'w'}\frac{\partial u}{\partial z}dz-\rho_0\overline{w'\left(\frac{p'}{\rho_0}+\frac{c^2}{2}\right)}\bigg|_{z=0}\\ D_*&=\rho_0\int_{-h}^{0}\epsilon dz\end{aligned}\right\}, \tag{15}$$

then (13), into which (14) has been substituted, becomes

$$\frac{dT_s}{dt}=\frac{2}{h^2}[-(G-D)+Fh+R(h-\gamma^{-1})+\gamma^{-1}\mathrm{Re}^{-\gamma h}]. \tag{16}$$

It is through this substitution of (14) into (13) that the mechanism for convective mixing enters into the mechanical energy equation. Only for very low wind speeds or for large evaporation does the convective mixing become important.

Eq. (16) can be used to eliminate dT_s/dt from the heat equation (12):

$$H\left(w+\frac{dh}{dt}\right)$$
$$=\frac{2[G-D+R\gamma^{-1}(1-e^{-\gamma h})]-h[F+R(1+e^{-\gamma h})]}{h(T_s-T_{-h})}. \tag{17}$$

The complete set of equations defining the upper

mixed layer is now expressed explicitly in terms of parameters which can be measured or can be estimated from measurements. Using (11), (16) and (17) with (9) substituted into (16) and (17), one obtains for the model the following set of first-order ordinary differential equations in h, T_s, and T_{-h}:

$$\frac{dT_s}{dt}=\frac{2}{h^2}[-(G-D)+h(B+H_e+H_s)+R(h-\gamma^{-1}+\gamma^{-1}e^{-\gamma h})], \tag{18}$$

$$H\left[w+\frac{dh}{dt}\right]=\frac{2[G-D+R\gamma^{-1}(1-e^{-\gamma h})]-h[B+H_e+H_s+R(1+e^{-\gamma h})]}{h(T_s-T_{-h})}, \tag{19}$$

$$\frac{d}{dt}T_{-h}=\gamma\,\mathrm{Re}^{-\gamma h}-(w+dh/dt)\left.\frac{\partial T}{\partial z}\right|_{-h}. \tag{20}$$

As the temperature gradient below the layer, $\partial T(z)/\partial z$, varies with time because of solar heating and vertical advection, $\partial T(z)/\partial z$ must be known for any time t in order to evaluate $\partial T(-h)/\partial z$ in (20). Eq. (10) provides the means for evaluating $T(z)$ and hence $\partial T/\partial z$ in the region $z\leqslant -h$.

Except for H, the Heaviside step function defined earlier, and γ, the extinction coefficient, all the coefficients in (18), (19) and (20) explicitly depend on the time t, as they are either dependent variables (h,T_s,T_{-h}) or time-varying inputs. The "forcing functions", which are directly related to processes either acting at the boundaries or originating beyond the boundaries, all occur on the right-hand side of the equations: they are G, the rate of turbulent energy production by the wind stress acting at the upper boundary; D, the total dissipation within the layer; R, the incident solar radiation; w, the imposed vertical velocity at the bottom of the layer; and B, H_e, H_s, the heat transfers at the air-sea interface.

The model represented by Eqs. (10), (18), (19) and (20) is similar to that of Kraus and Turner (1967). However, to obtain quantitative results on time scales of days (rather than months), the boundary conditions have been formulated more precisely: first, an arbitrary density (temperature) profile is specified below the mixed layer, and second, the penetration of solar radiation below the layer is included. In the results to be presented, the effects of these changes along with the effects of varying the meteorological inputs will be illustrated.

3. Properties of the equations

The set of coupled equations (10), (18), (19) and (20) would not be expected to have analytic solutions except in special instances. Further, the properties of this system of equations change drastically according to the value of the Heaviside step function H in (19) [0 for $w+(dh/dt)\leqslant 0$; 1 for $w+(dh/dt)>0$]. For any given set of boundary conditions imposed at some time t, the system is either in a wind-dominated or a heat-dominated regime, depending on whether the Heaviside step function is equal to 1 or 0, respectively.

For the wind-dominated regime ($H=1$), the entrainment mixing term is included in the equations so they retain their original form. Under these conditions, colder water from below is entrained into the mixed layer as a result of work done by the turbulence against the buoyancy forces. The layer, then, should increase in thickness and decrease in temperature. In this form, (19) and (20) can be integrated numerically by a Runge-Kutta technique for systems of ordinary differential equations; T_{-h} is evaluated from (10) and (20) at each time step and then substituted into (18) and (19).

For the heat dominated regime ($H=0$), the term representing the entrainment mixing at the bottom of the layer, $(w+dh/dt)(T_s-T_{-h})$, does not appear in the equations. Solar heating is greatest near the surface so the heat must be redistributed evenly throughout the mixed layer. In the heat-dominated regime, all the available turbulent energy is used in mixing the lighter warm water near the surface evenly throughout the layer and none remains to mix the bottom interface downward. The thickness of the mixed layer should therefore either remain unchanged, or, under extreme heating with very low winds, a new shallower layer of warm water should develop, superimposed on the old one.

By setting $H=0$ in (19), one obtains a single nonlinear equation in h:

$$(G-D)+R\gamma^{-1}(1-e^{-\gamma h}) =\tfrac{1}{2}h[R(1+e^{-\gamma h})+B+H_e+H_s]. \tag{21}$$

This equation can be solved numerically for h by a Newton's iterative technique (Henrici, 1964). Using the value of h so obtained, one can determine T_s by integration of (18) [with $G-D$ eliminated by use of (21)] over an appropriate time step:

$$\Delta T_s=[R(1-e^{-\gamma h})+B+H_e+H_s]\Delta t/h. \tag{22}$$

The transition between a wind-dominated and a heat-dominated regime occurs smoothly (in either direction) and is a function of the time-dependent behavior of the boundary conditions. In the numerical calculations, the system was assumed to be initially in the wind-dominated regime ($H=1$). If $w+(dh/dt)<0$ after the

iterations for a single time step had been carried out, then the calculations for that step were redone with the system in the heat-dominated regime ($H=0$). The time step used depended on the boundary conditions; usually it was 1 hr for the heat-dominated regime. For the wind-dominated regime, 1-min iteration steps were necessary.

4. Solutions for the wind-dominated regime

In this section solutions of the model in the wind-dominated regime are presented for boundary inputs constant in time to indicate the rate of deepening of the mixed layer during high winds. The relative importance on the rate of deepening of changes in the amount of available turbulent energy, in the stratification or stability below the layer, and in the radiative heating is indicated.

The solution for a wind obeying a normal distribution in time is also presented.

a. The concept of "mixing energy"

The turbulent energy input by the wind stress, G_*, as defined by (15), may be specified explicitly in terms of the wind stress τ. The rate of working by the wind stress at 10 m height is given by $E_a=\tau\bar{U}_{10}=\rho_a C_{10}\bar{U}_{10}^3$, where C_{10} is the drag coefficient, $\bar{U}_{10}$ the mean wind speed, and ρ_a the density of air. On the assumption that the wind and wave fields are statistically stationary, the same wind stress τ acts on the water below; a velocity scale appropriate to the underlying water is then

$$w_*=(\tau/\rho_0)^{\frac{1}{2}}=(\rho_a/\rho_0)^{\frac{1}{2}}C_{10}^{\frac{1}{2}}\bar{U}_{10}. \tag{23}$$

Eq. (23) can be used to estimate the rate of turbulent energy transfer downwards some depth below the surface:

$$E_w\approx w_*\tau=(\rho_a/\rho_0)^{\frac{1}{2}}C_{10}^{\frac{1}{2}}\bar{U}_{10}\tau=(\rho_a/\rho_0)^{\frac{1}{2}}C_{10}^{\frac{1}{2}}E_a. \tag{24}$$

This relation is consistent with the suggestion of Turner (1969) that the turbulent energy available for mixing within the layer is produced at a rate that is approximately a constant fraction m of the rate of downward transfer of turbulent energy from the wind field at 10 m:

$$G_*-D_*=m\bar{U}_{10}\tau=mE_a. \tag{25}$$

Values of m can be estimated from the rate of increase of potential energy in the water column calculated from temperature profiles of the upper ocean taken before and after a storm.

b. Analytic solution

For the simple case of no heat exchanges, no dissipation, and no imposed vertical velocity ($R=B=H_e=H_s=D=w=0$), it has been possible to obtain an analytic solution for the wind-dominated regime with a constant wind and a linear temperature profile, $L=\partial T/\partial z$, below the mixed layer.

With the above assumptions, (18), (19) and (20) can be combined into a single equation:

$$h''+bh(h')^3=0, \tag{26}$$

where $b=L/2G$ and $(\ )'=d(\ )/dt$. An exact analytic solution can be obtained if the substitution $y=h'$ is made in (26):

$$dy/dh+bhy^2=0. \tag{27}$$

A single integration yields

$$2=h'(bh^2+c_1), \tag{28}$$

and a second integration gives the following cubic equation in h as a function of t:

$$h^3+\frac{3c_1h}{b}+\left(-\frac{6t}{b}+\frac{3c_2}{b}\right)=0. \tag{29}$$

The constants of integration, c_1 and c_2, can be evaluated from the initial conditions

$$c_1=2\left(\frac{dh}{dt}\bigg|_{t=0}\right)^{-1}-bh_0,\quad c_2=-h_0\left(c_1+\frac{bh_0^2}{3}\right). \tag{30}$$

The cubic equation given by (29) is already in the reduced form, $x^3+px+q=0$, so that the roots can be evaluated directly by Cardan's formulae (see Beaumont and Pierce, 1963).

When $(p/3)^3+(-q/2)^2>0$, there exists one real root and a pair of complex conjugate roots. The appropriate root must necessarily be the real one:

$$h=\left\{-\frac{q}{2}+\left[\left(\frac{q}{2}\right)^2+\left(\frac{p}{3}\right)^3\right]^{\frac{1}{2}}\right\}^{\frac{1}{3}}+\left\{-\frac{q}{2}-\left[\left(\frac{q}{2}\right)^2+\left(\frac{p}{3}\right)^3\right]^{\frac{1}{2}}\right\}^{\frac{1}{3}}. \tag{31}$$

The same equation also gives the root of interest when

$$\left(\frac{p}{3}\right)^3+\left(\frac{-q}{2}\right)^2=0.$$

For the case $(p/3)^3+(-q/2)^2<0$, there are three solutions:

$$h=2\left(\frac{-p}{3}\right)^{\frac{1}{2}}\cos\left(\frac{\phi}{3}+120n\right), \tag{32}$$

one for each of n equal to 0, 1 and 2, where

$$\phi=\cos^{-1}\left[\left(\frac{-q}{2}\right)\Big/\left(\frac{-p^3}{27}\right)^{\frac{1}{2}}\right].$$

The appropriate solution, the one with $n=0$, is found by matching the solution with that from (31) as $(p/3)^3+(-q/2)^2\to 0$. For a typical case, (32) is the

TABLE 1. Model results for the constant input mixing regime. [G_*-D_* is the wind energy available for mixing; R_* and $-B_*$ are the solar and back radiation at the sea surface; $-\partial T/\partial z$ is the temperature gradient immediately below the layer; Ts_t is the sea surface temperature at time t (hr); and h_t is the thickness of the mixed layer.] Ts_0 and h_0 were 10 m and 8.5C, the extinction coefficient γ was 0.002 cm^{-1}, and the drag coefficient C_{10} was 0.0013.

Run	G_*-D_* (ergs cm^{-2} sec^{-1})	R_* (cal cm^{-2} day^{-1})	B_* (cal cm^{-2} day^{-1})	$-\partial T/\partial z$ (°C m^{-1})	Ts_{24} (°C)	Ts_{48} (°C)	h_{24} (m)	h_{48} (m)
1	3.05	0	0	0.0385	7.75	7.53	37.1	47.8
2	6.10	0	0	0.0385	7.53	7.26	47.8	61.2
3	3.05	400	−80	0.0385	7.90	7.78	34.5	43.1
4	3.05	0	0	0.0192	7.86	7.71	43.9	57.8

solution for times less than several hours, but (31) becomes the solution for times greater than several hours.

For large times, the expression (31) becomes (with the model parameters substituted for p and q)

$$h \to \left(\frac{6t}{b}\right)^{\frac{1}{3}} = \left(\frac{12G}{L}\right)^{\frac{1}{3}} t^{\frac{1}{3}}. \tag{33}$$

This limiting form provides insight into the dependence of the mixing model on certain thermocline parameters. For large t, the depth depends on the one-third power of the mixing energy; thus, it depends linearly on the wind speed. This simple relationship gives some theoretical justification to the empirical result of Tabata *et al.* (1965) that the depth of the mixed layer is linearly related to the wind speed averaged over the previous 12-hr period. That the depth depends on the ratio G/L is not surprising since G represents the mixing energy available, and the temperature gradient L is proportional to the buoyancy forces against which work is done. The expression (33) is, in fact, identical in form to the following expression derived by Kato and Phillips (1969) using a potential energy argument for a constant stress and a linear density profile:

$$h(t) = w_*\left(\frac{15t}{N_0^2}\right)^{\frac{1}{3}}, \tag{34}$$

where $N_0^2 = -g\partial\rho/\partial z$.

In the tank experiment of Kato and Phillips, there was no mixed layer initially, only a linear density profile. In the present model, the layer thickness and the density difference at the bottom of the layer are independently specified as initial conditions. At large times, however, the initial conditions become unimportant and the two systems become equal in the limit.

In a similar laboratory experiment of a turbulent layer penetrating into a stably stratified fluid, Moore and Long (1971) also found that the entraining interface descended at the rate of $t^{\frac{1}{3}}$. The turbulence in their experiment was generated by a series of slanted jets directed at the surface of the fluid.

c. *Numerical solutions*

The system of equations (18), (19) and (20) (with $H=1$) was solved numerically when solar heating was included, or when the inputs varied in time, as analytic solutions could not be found in such cases. A numerical solution obtained for the case just discussed was checked against the analytic solution: both gave the same answers provided that time steps less than an hour were used in the numerical calculations.

Results of the numerical integrations for the wind-dominated regime with several different values for the input parameters (given in Table 1) are presented in Fig. 3. The temperature profiles in the lower panel correspond to Run 1; the value used for the mixing energy is appropriate to a constant wind speed $\tilde{U}_{10}$ of about 12.5 m sec^{-1} (except for Run 2, where it is appropriate to a wind speed of about 17 m sec^{-1}).

These results for the wind-dominated regime illustrate three main points. First, doubling the mixing energy in Run 2 produced a sizable increase (almost 30%) in the layer thickness from Run 1. Second, decreasing the stratification by a factor of 2 in Run 4 (from Run 1) had a smaller but nevertheless noticeable effect on the layer thickness. Third, solar heating of 400 cal cm^{-2} day^{-1} and surface back radiation of −80 cal cm^{-2} day^{-1} (both typical of a summer day at mid-latitudes) did not have an appreciable effect on the thickness of the mixed layer as shown in Run 3. During the winter, however, large evaporative heat losses at the sea surface often accompany high winds, resulting in intense convective mixing which may have a more appreciable effect on the wind-dominated regime than in the case just investigated.

In Run 1, the rate at which turbulent energy from the wind becomes available for mixing within the layer, $G_*-D_*=m\tilde{U}_{10}\tau$, was calculated with m set equal to 0.0012. This corresponds to a scale velocity, $m\tilde{U}_{10}$, equal to w_*, the friction velocity in the water [defined in Eq. (26)]. According to (33), doubling m or doubling the rate of availability of mixing energy as in Run 2, increases the limiting depth of the mixed layer by 25–30%. As the thickness of the mixed layer during a storm can be determined from observations to within 20%, this result indicates that physically realistic

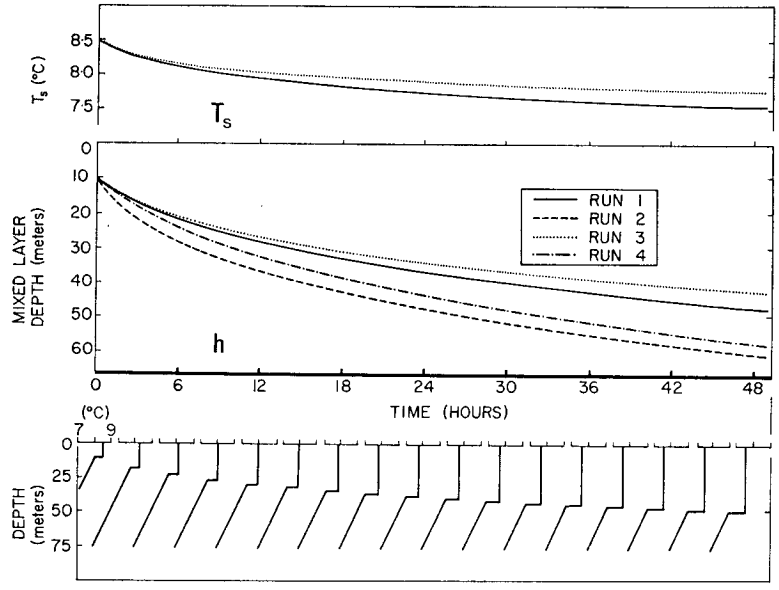

FIG. 3. Results of the model for a constant wind. Run 1: $G_*=3.05$ ergs cm^{-2} sec^{-1}; $R_*=B_*=0$, $\partial T/\partial z=0.0385$C m^{-1}; Run 2: $G_*=6.1$ ergs cm^{-2} sec^{-1}; Run 3: $R_*=400$ cal cm^{-2} day^{-1}, $B_*=-80$ cal cm^{-2} day^{-1}; Run 4: $\partial T/\partial z=0.0192$C m^{-1}. In Runs 2, 3, and 4, parameters not mentioned above are unchanged from Run 1. $G_*=3.05$ ergs cm^{-2} sec^{-1} corresponds to a mean wind speed of 12.5 m sec^{-1}.

solutions are obtained only for values of m differing by less than a factor of 2. Kato and Phillips (1969) obtained an empirical value for m of 0.0015 with an uncertainty of about 30%. The value $m=0.01$, estimated by Turner (1969) from two cases of salinity-temperature-depth profiles in the open ocean, is too large to allow this model to yield realistic deepening.

The behavior of the model for a time-varying wind is illustrated in Fig. 4. The wind speed followed a normal curve in time (with a maximum amplitude of 15 m sec^{-1} and a standard deviation of 18 hr) representing a storm or gale lasting several days. The variable parameters and the initial temperature profile were approximately equal to those in Run 1. There were no heat exchanges.

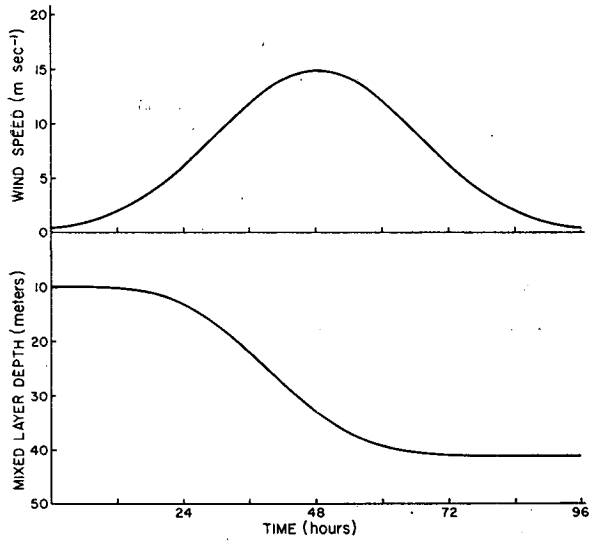

FIG. 4. Deepening of the mixed layer for a Gaussian-shaped (in time) wind function. The mixing parameters and the initial conditions are similar to those in Run 1 of Fig. 3.

5. Solutions for the heat-dominated regime

The heat-dominated regime is represented by Eq. (21) in which there is no explicit time dependence. Therefore, for inputs constant in time, the mixed layer thickness h is also constant in time, and the mixed layer temperature T_s, obtained from (22), increases linearly with time.

With the assumptions $H_e=H_s=w=0$, calculations were carried out to determine the sensitivity of the heat-dominated regime to the value used for γ, the extinction coefficient of solar radiation in sea water, and to the mechanisms by which the net radiative heat exchange was achieved. The results of these calculations for a wind speed of 4 m sec^{-1} are summarized in Table 2.

TABLE 2. Heating regime with constant inputs. The wind speed was 4 m sec^{-1} corresponding to a mixing energy $G_*-D_*=0.123$ ergs cm^{-2} sec^{-1} [R_* and $-B_*$ are the solar and back radiation at the sea surface; γ is the extinction coefficient of the solar radiation; h_1 is the mixed layer depth when the solar radiation below the layer is neglected; and h_2 is the mixed layer depth when it is included.]

Run	R^* (cal cm^{-2} day^{-1})	B^* (cal cm^{-2} day^{-1})	γ (cm^{-1})	h_1 (m)	h_2 (m)
1	350	0	0.002	14.1	12.2
2	350	0	0.001	24.1	—
3	440	−90	0.002	16.7	15.2

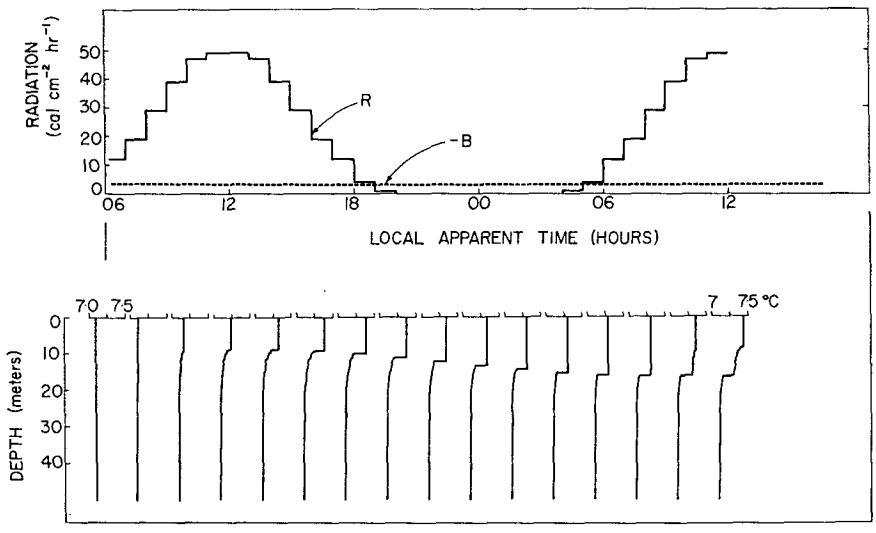

FIG. 5. Results of the model with diurnal heating for 30 hr. The daily total solar radiation and back radiation are 400 and -80 cal cm^{-2} day^{-1}. The wind speed is 4 m sec^{-1}.

The largest effect evident in Table 2 is that obtained in Run 2, where the extinction coefficient γ was changed to 0.001 cm^{-1} from 0.002 cm^{-1} in Run 1. Decreasing γ by a factor of 2 (allowing the solar radiation to penetrate to greater depths) increased the mixed layer thickness by 70%. The values used here for the total extinction coefficient are typical of the northeast Pacific Ocean during the summer months when there is an increased amount of phytoplankton in the upper layer (Table 1 in Parsons *et al.*, 1966).

In Runs 1 and 3, the mixed layer depth was calculated first where the solar heating had been confined to the upper layer, and second where the extinction term had been retained in the layer below. Where the radiative transfer below the mixed layer was neglected, the mixed layer thickness was over-estimated by about 15%. Comparison of the depths obtained in Runs 1 and 3 shows that the back radiation should be included explicitly in the model. In Run 1, all the heat exchange was by solar heating; in Run 3, the same total heat exchange was composed of solar heating penetrating the whole layer and of longwave radiational cooling from the sea surface. The net result of specifying the back radiation separately was to increase the thickness of the mixed layer by about 25%.

6. Solutions for diurnal heating

The most obvious meteorological phenomenon with a time scale of 1–5 days is the daily cycle in the incoming solar radiation. In this section, diurnally varying solar heating is applied to the model for several wind speeds. The resulting response of the mixed layer is presented to illustrate further the time-dependent properties of the model and to determine the maximum magnitude of the daily fluctuation in sea surface temperature to be expected in the open ocean.

a. Typical daily cycle

The response of the surface layer of the ocean to diurnally varying solar radiation ought to be a maximum for intense solar heating and low wind speeds. As an example of typical summer heating in the open ocean, consider Ocean Station *Papa*: from the Canadian Monthly Radiation Summary (1970), the average daily solar radiation at *Papa* in May and June, 1970, was 367 cal cm^{-2} day^{-1}, and from the tables of Laevastu (1963), 12-hr averages for back radiation at *Papa* have been calculated for the same period which have an overall average of -82 cal cm^{-2} day^{-1}. Therefore, as input into the model, a daily total solar radiation of 400 cal cm^{-2} day^{-1}, composed of hourly values distributed as shown in the upper panel of Fig. 5, and a constant back radiation of -80 cal cm^{-2} day^{-1} were used. With the large relative humidities (over 85%) and the small air-sea temperature differences usually observed at *Papa* during the summer months, the turbulent heat flux, H_e+H_s, is usually less than half the back radiation and was ignored.

The resulting behavior of the upper mixed layer for a 30-hr period is presented in the lower panel of Fig. 5 for a constant wind speed of 4 m sec^{-1}. The profiles plotted every 2 hr show that a shallow layer of warm water built up during the day until about 1600 local time. At that time, the solar heating had decreased sufficiently for the layer to start mixing downward. The layer descended from about 8 m to a maximum depth of about 16 m at 0600 local apparent time. During the second day, a new warm layer again started to build up superimposed on the previous day's layer. The structure below was affected only slightly by the small fraction of solar radiation which penetrates below the active mixed layer. The step structure appearing below the

TABLE 3. Model results for the diurnal heating at various wind speeds. [$\bar{U}_{10}$ is the wind speed; h_{min} and h_{max} are the minimum and maximum thicknesses of the diurnally varying mixed layer; h_c is the mixed layer thickness for constant heating; $\Delta T_{96\ hr}$ is the increase in sea surface temperature after 96 hr; and $\Delta T_{diurnal}$ is the amplitude of the diurnal variation (with the trend removed) of the sea surface temperature.] The extinction coefficient γ was 0.002 cm^{-1}, and the available mixing energy coefficient m was 0.0012.

Run	$\bar{U}_{10}$ (m sec^{-1})	h_{min}	h_{max} (m)	h_c	$\Delta T_{96\ hr}$	$\Delta T_{diurnal}$ (°C)
1	0.0	3.86	7.92	7.90	1.27	±0.27
2	4.0	8.64	16.28	16.24	0.80	±0.19
3	8.0	21.86	52.49	52.46	0.26	±0.09

mixed layer resulted because the solar heating was applied as hourly values.

b. Effects of wind speed

Results of the diurnal heating model for different wind speeds are shown in Fig. 6 and summarized in Table 3. Each run was for a 4-day period. The heat input was the same as in Fig. 5, but the wind speed was 0, 4 and 8 m sec^{-1}. The traces in the middle plot of Fig. 6 represent the depth of the active interface, $z = -h$, as a function of time. The temperature profiles, plotted every 6 hr at the bottom of the figure, are for the intermediate wind speed of Run 2 (which corresponds to the case shown in Fig. 5). They indicate that while the upper mixed layer thickness oscillated markedly during each day, the formation of the main temperature step (at about 16 m) occurred at the maximum depth to which the diurnal effects penetrated. As one would expect, at higher winds the layer penetrated to greater depths and its thickness had a marked diurnal oscillation, but the mean temperature increase and the diurnal variation in sea surface temperature were correspondingly smaller. The layer depths for the three runs, calculated for the same daily solar heat input but put into the layer at a constant rate, are given in Table 3 under h_c. The maximum layer thickness for diurnal heating was about the same as the thickness obtained for constant heating.

The results for the zero wind case (Run 1) must be interpreted with great caution. During the night, the solar radiation R is zero so that for zero winds, only the back radiation at the sea surface, $-B$, drives the mixing. Under these conditions, Eq. (19) for the rate

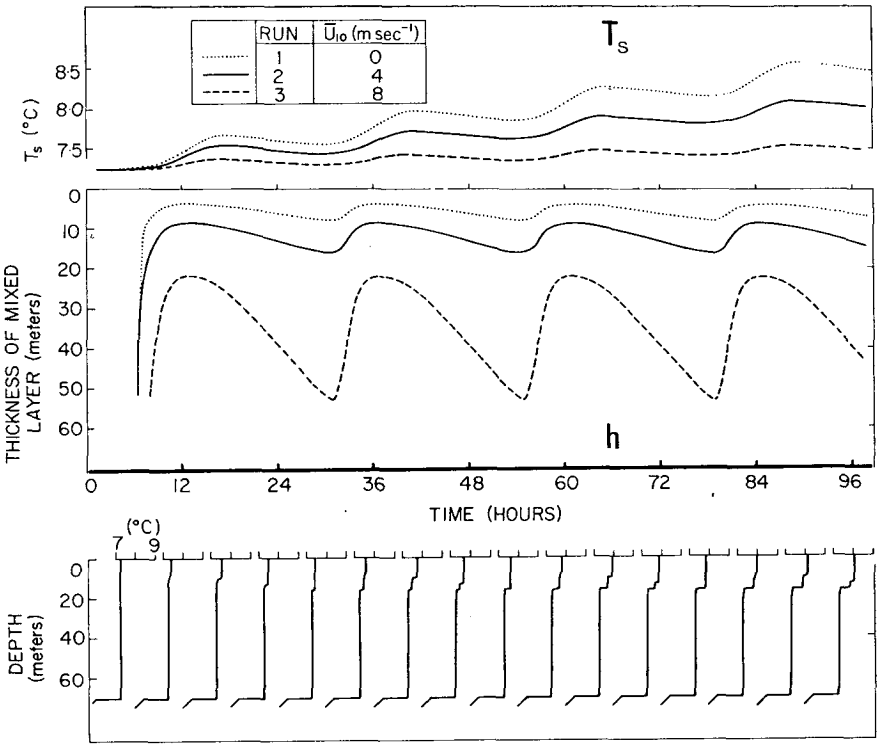

FIG. 6. Results of the diurnal heating for 4 days with different wind speeds. Run 2, for which the temperature profiles are plotted, is the same case illustrated in Fig. 5. The heat input is identical with that in Fig. 5.

of thickening of the mixed layer becomes

$$\frac{dh}{dt}=\frac{-2D-hB}{h(T_s-T_{-h})}, \tag{19a}$$

indicating that the layer thickens at a rate dependent upon the amount of convective energy (generated by $-B$) that is not dissipated within the layer. However, through the parameterization of the mixing energy generated by the wind stress [Eq. (25)], the dissipation D was effectively set equal to zero when the wind speed was set equal to zero. While this parameterization is suitable for larger wind speeds (when the convective energy is negligible compared to the wind-generated mixing energy), the dissipation is almost certainly important in balancing any convective mixing at zero wind speed.

Therefore, the effect of neglecting dissipation at low wind speeds was to give a larger-than-expected diurnal oscillation in both sea surface temperature and mixed layer thickness. Nevertheless, the diurnal oscillation (with the trend removed) obtained in Run 1 for zero wind speed was only ±0.27C, a difference which would be difficult to measure with any confidence in the open ocean. The diurnal oscillation for 8 m sec^{-1} winds was ±0.09C, a difference which definitely would not be observable in the open ocean. At low wind speeds and large solar heating, the small diurnal effect in the sea surface temperature would be further masked out by the horizontal "patchiness" and the high temperature gradients near the surface that tend to develop under such conditions. The conclusion to be drawn from the model then is that diurnal effects in the upper mixed layer of the open ocean would usually be too small to be observed.

7. Conclusions

A one-dimensional theoretical model has been developed to describe the time-dependent behavior of the upper layer of the ocean caused by meteorological influences acting over times of 1–5 days. For the case of constant winds and no heat exchanges, an analytic solution for the mixing entrainment has been obtained. The solution for large times [Eq. (33)] indicates that the eventual depth of the mixed layer depends equally on G, the amount of turbulent energy produced by the wind stress that becomes available for mixing, and on L, the temperature gradient below the layer (which is a measure of the stratification or buoyancy forces encountered by the mixing). The rate of deepening is found to be proportional to (time)$^{\frac{1}{2}}$ consistent with empirical results obtained both in the laboratory and in the open ocean. The numerical results indicate that for typical summer conditions, the heat exchanges are relatively unimportant in determining the layer thickness at high wind speeds.

Under conditions of low wind speeds and substantial solar heating, however, the thickness of the mixed layer is extremely sensitive to the value used for the extinction coefficient of the solar radiation, a parameter which varies by at least a factor of 2 according to the amount of phytoplankton present in the upper layer. Lesser effects are caused by changes in the relative amounts of solar heating and heat exchanges at the sea surface. The response of the model to a diurnal heating cycle indicates that the daily fluctuations in sea surface temperature would usually be too small to be measured in the upper ocean. The limitations of the model for very low wind speeds do not severely restrict its usefulness in describing the seasonal thermocline in the open ocean as the average wind speed there during the summer months is still typically 7–8 m sec^{-1}.

The results of the model for a Gaussian-shaped "storm" of several days' duration together with the results for diurnally varying heating indicate that the model should be successful in simulating the time-dependent behavior of the mixed layer in the open ocean on time scales of 1 day to about 1 week. Such a simulation is the object of a companion paper by Denman and Miyake (1973) for a series of observations obtained at Ocean Station *Papa*.

Acknowledgments. The author would like to thank his research supervisor, Dr. M. Miyake, for advice and support during this study. Drs. R. W. Burling and R. W. Stewart also provided helpful criticisms and comments. The National Research Council of Canada provided financial support both personally to the author and for the computing facilities.

REFERENCES

Beaumont, R. A., and R. S. Pierce, 1963: The *Algebraic Foundations of Mathematics*. Reading, Mass., Addison-Wesley, 486 pp.

Bryan, Kirk, 1969: Climate and the ocean circulation: III. The ocean model. *Mon. Wea. Rev.*, **97**, 806–827.

Canadian Monthly Radiation Summary, 1970: Meteorological Branch, Department of Transport.

Denman, K. L., and M. Miyake, 1973: Upper layer modification at Ocean Station 'Papa': Observations and simulation. *J. Phys. Oceanogr.*, **3**, 185–196.

Ekman, V. W., 1905: On the influence of the earth's rotation on ocean currents. *Ark. Mat. Astron. Fys.*, **2**, No. 11.

Geisler, J. E., and E. B. Kraus, 1969: The well-mixed Ekman boundary layer. *Deep-Sea Res.*, **16** Suppl., 73–84.

Grant, H. L., A. Moilliet and W. M. Vogel, 1968: Some observations of the occurrence of turbulence in and above the thermocline. *J. Fluid Mech.*, **34**, 443–448.

Henrici, Peter, 1964: *Elements of Numerical Analysis*. New York, Wiley, 336 pp.

Jerlov, N. G., 1968: *Optical Oceanography*. London, Elsevier, 199 pp.

Kato, H., and O. M. Phillips, 1969: On the penetration of a turbulent layer into a stratified fluid. *J. Fluid Mech.*, **37**, 643–655.

Kitaygorodskiy, S. A., 1961: On the possibility of theoretical calculation of vertical temperature profile in upper layer of the sea. *Izv. Akad. Nauk SSSR, Ser. Geofiz.*, No. 1–6, 313–318.

Kraus, E. B., and J. S. Turner, 1967. A one-dimensional model of the seasonal thermocline: II. The general theory and its consequences. *Tellus*, **19**, 98–106.

Laevastu, T., 1963: Energy exchange in the North Pacific, Part I. Formulas and nomographs. Rept. 29, Hawaii Institute of Geophysics.

Manabe, Syukuro, 1969: Climate and the ocean circulation: I. The atmospheric circulation and the hydrology of the earth's surface, II. The atmospheric circulation and the effect of heat transfer by ocean currents. *Mon. Wea. Rev.*, **97**, 739–805.

Moore, M. J., and R. R. Long, 1971: An experimental investigation of turbulent stratified shearing flow. *J. Fluid Mech.*, **49**, 635–655.

Munk, W. H., and E. R. Anderson, 1948: Notes on a theory of the thermocline. *J. Marine Res.*, **7**, 276–295.

Namias, J., 1969. Autumnal variations in the North Pacific and North Atlantic anticyclones as manifestations of air-sea interactions. *Deep-Sea Res.*, **16** Suppl., 153–164.

——, 1970: Macroscale variations in sea-surface temperatures in the North Pacific. *J. Geophys. Res.*, **75**, 565–582.

Parsons, T. R., L. F. Giovando and R. J. LeBrasseur, 1966: The advent of the spring bloom in the eastern subarctic Pacific Ocean. *J. Fish. Res. Bd. Canada*, **23**, 539–546.

Phillips, O. M., 1966: *The Dynamics of the Upper Ocean*. Cambridge University Press, 261 pp.

Tabata, S., N. E. J. Boston and F. M. Boyce, 1965: The relationship between wind speed and summer isothermal surface layer of water at Ocean Station P in the eastern subarctic Pacific Ocean. *J. Geophys. Res.*, **70**, 3867–3878.

Turner, J. S., 1969: A note on wind mixing at the seasonal thermocline. *Deep-Sea Res.*, **16** Suppl., 297–300.

——, and E. B. Kraus, 1967: A one-dimensional model of the seasonal thermocline. I. A laboratory experiment and its interpretation. *Tellus*, **19**, 88–97.